Interactions of strongly coupled superconducting microbridges

R. Escudero and H. J. T. Smith
Guelph-Waterloo Program for Graduate Work in Physics, Waterloo Campus, University of Waterloo, Waterloo, Ontario, Canada, N2L 3G1

(Received 20 April 1984; accepted for publication 8 June 1984)

An electronic analog simulation of two coupled superconducting microbridges is shown to give similar results to the numerical solution. For strongly coupled microbridges some new phenomena are revealed. Strongly coupled thin-film microbridges were prepared by a new technique and their current-voltage characteristics confirm some of the predictions that are indicated by the analog simulation.

INTRODUCTION

Superconducting microbridges have been intensively studied in the past few years. The resistivity shunted junction (RSJ)[1,2] model, which consists of an ideal Josephson element in parallel with a resistance, has been shown to well represent the equilibrium properties of superconducting microbridges. With so much interest in developing superconducting logic elements[3] and in Josephson junction arrays[4] there has been a need to study the coupling that takes place when two microbridges are in a close proximity. This problem has been theoretically and experimentally studied.[5–8] Coupling due to the order parameter modulation may occur when the separation of the microbridges is less than the coherence length. This problem is discussed by Howard *et al.*[9] and Way *et al.*[10] Quasiparticle coupling will occur when the separation of the microbridges is less than the quasiparticle diffusion length. This problem is discussed by Nerenberg *et al.*[5] who represented two microbridges by the RSJ model and the coupling between the microbridges by a shunt resistance. The use of a shunt resistor to represent the coupling was justified by Jillie *et al.*[6] in the case when the coupling is caused by quasiparticles. Nerenberg *et al.*[5] were able to analyze the two coupled microbridges by a numerical method, although their procedure consumed much computer time. They also solved the problem by a less exact perturbation method. The interaction of the microbridges is dependent on parameters such as the coupling strength and the relative critical currents of the two microbridges. To investigate the coupled microbridges over the full range of these parameters by numerical methods would require a great deal of computer time. Electronic analogs[11–18] of microbridges have been developed recently and whilst these electronic analogs usually do not have the accuracy of digital simulation, they are much quicker and less expensive. In this paper we describe the use of an electronic analog to solve the problem of microbridges coupled by quasiparticles.

COUPLED MICROBRIDGE EQUATIONS

The circuit shown in Fig. 1 is governed by the following coupled differential equations:

$$V_1 = \left(1 - \frac{\alpha^2}{\delta}\right)(I_1 - I_{c1}\sin\phi_1) + \frac{\alpha}{\delta}V_2, \tag{1}$$

$$\frac{1}{\delta}V_2 = \left(1 - \frac{\alpha^2}{\delta}\right)(I_2 - I_{c2}\sin\phi_2) + \frac{\alpha}{\delta}V_1. \tag{2}$$

For convenience, normalized units have been used following the scheme of Nerenberg *et al.*[5] and

$$\alpha = \left(1 + \frac{R_s}{R_2}\right)^{-1}, \quad \delta = \left(1 + \frac{R_s}{R_1}\right)\Big/\left(1 + \frac{R_s}{R_2}\right),$$

$$\bar{i}_c = \frac{i_{c1} + i_{c2}}{2}, \qquad V_0 = \frac{\bar{i}_c R_1(R_2 + R_s)}{R_1 + R_2 + R_s},$$

$$I_{1,2} = \frac{i_{1,2}}{\bar{i}_c}, \qquad V_{1,2} = \frac{v_{1,2}}{V_0} = \frac{\hbar\dot{\phi}_{1,2}}{2eV_0}.$$

In the above i_1, i_2, i_{c1}, i_{c2}, v_1, and v_2 are the actual circuit currents and voltages. ϕ_1 and ϕ_2 are the phases across microbridges 1 and 2. These two equations have been solved using the electronic analog that is described below. The series aiding case has the same Eq. (1) and (2) but the sign of α is reversed.

ELECTRONIC ANALOG

A suitable electronic analog for an individual microbridge, based on a phase lock loop, has been described by

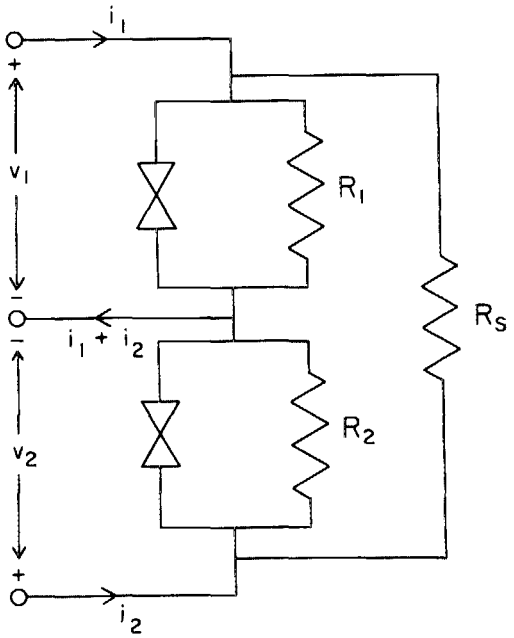

FIG. 1. Equivalent circuit of two coupled microbridges.

 0021-8979/84/233271-07$02.40

Henry *et al.*[11] It solves the RSJ model equations.

In Fig. 2, two of these circuits have been used to simulate a pair of microbridges. In essence this arrangement solves Eqs.(1) and (2). Quasiparticle coupling between the microbridges is introduced by way of the resistors r_1' and r_2'. The scheme of Henry *et al.*[11] has been followed with the exception of the reference oscillator, which here is a fixed frequency 100-kHz crystal oscillator followed by a Princeton Applied Research model 210 selective amplifier. The same reference signal was used for both circuits. A trimmer capacitor was placed parallel with the fixed capacitor of the voltage controlled oscillator and the circuit was set up by adjusting the trimmer capacitor instead of adjusting the reference oscillator frequency as was done in Ref. 11. Apart from this feature and the coupling resistors the circuits are identical to those described by Henry *et al.* The outputs of the two 741 op amps V_1 and V_2 are given by

$$V_1 = r_1(I_1 - I_{c1}\sin\phi_1) + \frac{r_1}{r_1'}V_2, \tag{3}$$

$$V_2 = r_2(I_2 - I_{c2}\sin\phi_2) + \frac{r_2}{r_2'}V_1, \tag{4}$$

and

$$\dot{\phi}_{1,2} = kV_{1,2}.$$

Equations (3) and (4) are analogous to Eqs. (1) and (2) when the following correspondences are made:

$$r_1 = 1 - \frac{\alpha^2}{\delta}, \quad r_2 = \delta\left(1 - \frac{\alpha^2}{\delta}\right),$$

$$r_1' = r_2' = \frac{\delta}{\alpha}\left(1 - \frac{\alpha^2}{\delta}\right).$$

The output of the electronic analog is in reduced units and in order to calibrate the output in terms of real units (volt, amp, and sec) it is necessary to know V_0. With the i_1 and i_2 direction as shown in Fig. 2, we have selected the series opposing case. The series aiding case is obtained simply by reversing direction of either i_1 or i_2. As a test, the circuit was set up to reproduce the results of the series aiding case that Nerenberg *et al.* displayed in their Fig. 2. This required $I_{c1} = 1.2$, $I_{c2} = 0.8$, $\delta = 0.667$, and $\alpha = 0.2$, $I_1 = 2$. In the electronic analog the quantities $V_{1,2}$, $I_{1,2}$ and $I_{c1,2}$, which are dimensionless, are represented by real voltages and currents. The magnitude of the voltage in the analog circuit that repre-

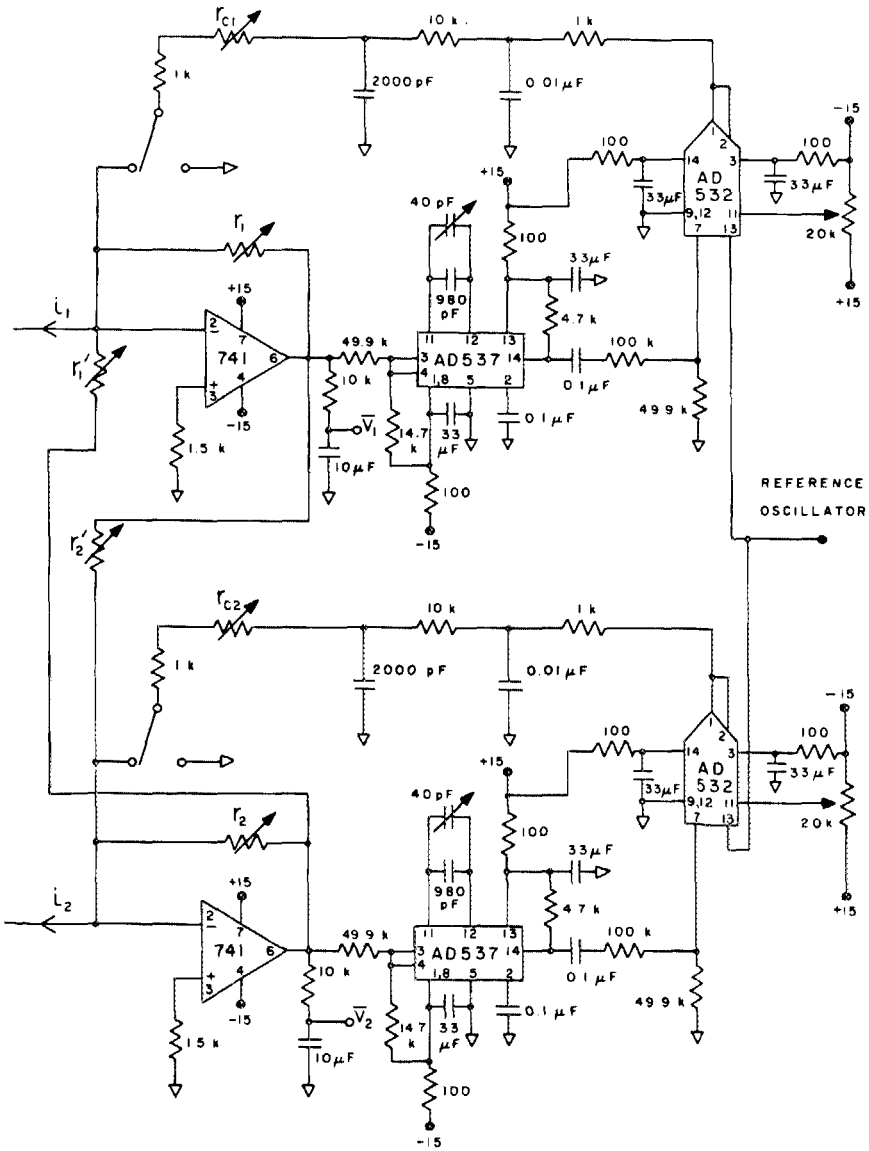

FIG. 2. Detailed circuit diagram of the electronic analog simulator for analyzing the circuit of Fig. 1.

sents one unit of $V_{1,2}$ was chosen to be 0.666 V. This choice is not quite arbitrary and the choice was made so that the circuit potentials would not on the one hand exceed their maximum allowable values whilst on the other hand they were as large as possible so that their measurement would have maximum accuracy. Similarly the magnitude of the current in the analog circuit that represents one unit of $I_{1,2}$ or $I_{c1,2}$ was chosen to be 66.7 μA. Consequently the resistance in the analog circuit that represents one unit of $r_{1,2}$ or $r'_{1,2}$ must be 10 000 Ω. In the electronic analog one unit of time represents $k\hbar/2eV_0$ seconds of real time where k is the voltage to frequency conversion factor of the voltage controlled oscillator and for these circuits was 13 360 rad/sec V. The electronic analog circuit was set up with $i_{c1} = 80\,\mu$A peak, $i_{c2} = 53\,\mu$A peak, $r_1 = 9.4$ kΩ, $r_2 = 6.27$ kΩ, $r'_1 = r'_2 = 31.33$ kΩ. $I_{c1,2}$ were set by adjusting $r_{c1,2}$ whilst monitoring $I_{c1,2}$ by measuring the potentials across the 1000-Ω resistors in series with $r_{c1,2}$. The result of the simulation is given in Fig. 3 for the series aiding case and in Fig. 4 for the series opposing case. The results agree within experimental error with those of Nerenberg *et al.* The output $\bar{V}_1$ and $\bar{V}_2$ are in the previously defined reduced units. The locking region which occurs when the potentials of the two microbridges are equal is clearly visible. However, it is slightly curved whereas the same region calculated by Nerenberg *et al.* is linear. Note in this connection that Jain *et al.*[7,19] show similar curvature in the locking region when a reactive element was included in series with the shunt resistor. A possible cause of the curvature in the locking region observed with the analog simulator may be the presence of spurious phase shifts in the analog simulation circuit. The harmonic locking regions that occur when $\bar{V}_1/\bar{V}_2 = 0.5,2,3$ are also visible in both the I_2-$\bar{V}_1$ and the I_2-$\bar{V}_2$ plots. A further check on the performance of this circuit was made by considering the coupling coefficient α. Jillie[20] found α to be given by the ratio I_{Q2}/I_{Q1} where I_{Q2} is given by $[\Delta I_{c2}$ (series) $-$ ΔI_{c2} (opposing)]/2. ΔI_{c2} is the change of the critical current from the uncoupled case. I_{Q1} is the quasiparticle current of microbridge 1. Critical current data was taken from Figs. 3 and 4. On substitution into Jillie's formula we found $\alpha = 0.195$. We conclude that the circuit of Fig. 2 is a good model for a coupled pair of microbridges.

Jain *et al.*[7] have carried out perturbation calculations and have also made experimental measurements of the locking in coupled microbridges. They have investigated the dependence of the overall potential across both microbridges as a function of the bias current. In the neighborhood of the locking region this dependence has a form similar to the current-voltage (I-V) characteristic predicted by the RSJ model for a single microbridge. In Fig. 5 I_2 vs $\bar{V}_2$-$\bar{V}_1$ has been plotted for the data of Fig. 3 and this data has been fitted to a hyperbolic-type equation as predicted by the RSJ model.

Away from the locking region other effects of the coupling occur. At large values of the current in microbridge 2 in the series aiding mode it is possible for the potential of microbridge 1 to be reduced to zero. When this occurs the potential of microbridge 1 remains at zero over a finite current range and the phase across microbridge 1 stays at a small value less than $pi/2$ although it oscillates at the same

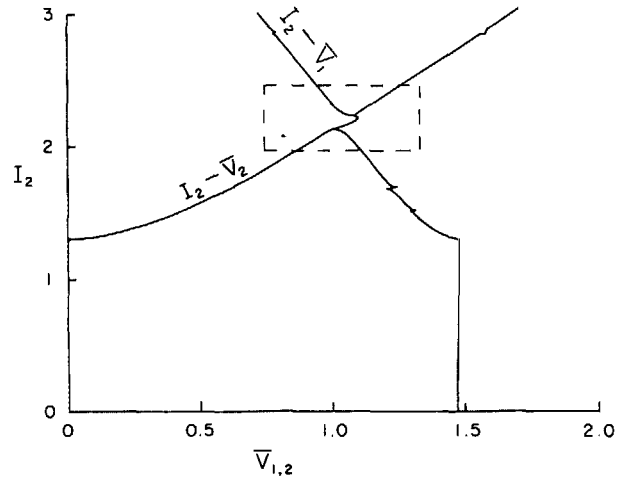

FIG. 3. Voltage characteristics from the analog simulator for $\alpha = 0.2$, $\delta = 0.667$, $I_1 = 2$, $I_{c1} = 1.2$, $I_{c2} = 0.8$, for the series aiding case.

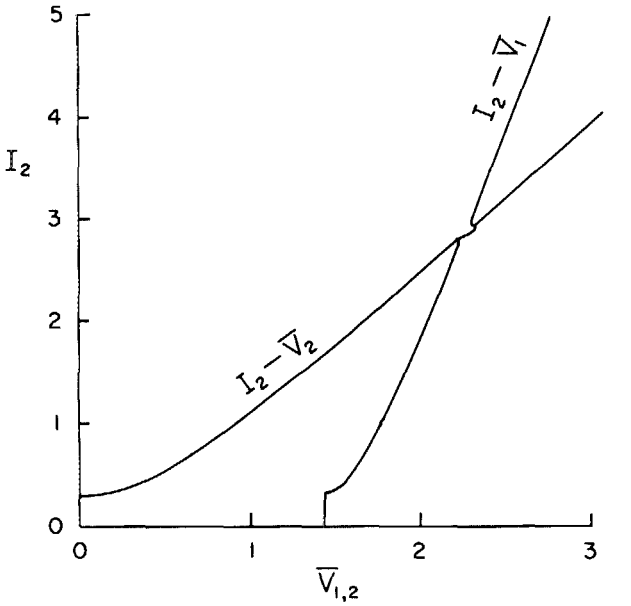

FIG. 4. Voltage characteristics from the analog simulator for the series opposing case and for the same parameters as Fig. 3.

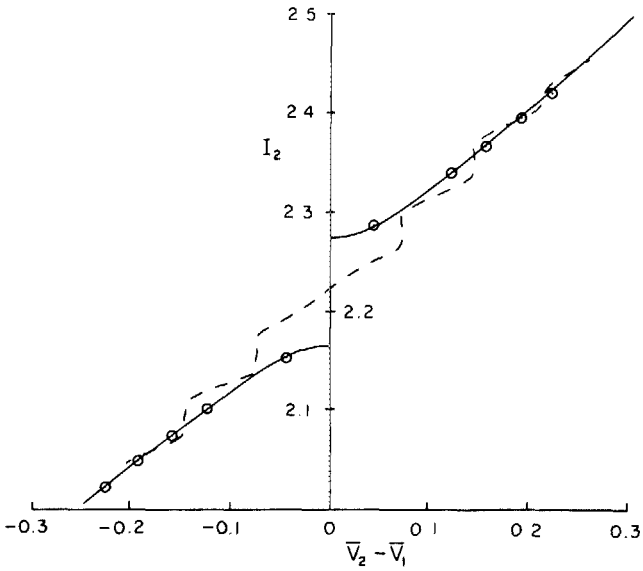

FIG. 5. I_2 vs $\bar{V}_2$-$\bar{V}_1$ for the data within the boxed region of Figs. 3 and 14. The dashed curve is the output for the identical conditions but in the presence of a 100-Hz ac signal. The amplitude of the ac signal was 0.25 (normalized units). The O's are points calculated from the RSJ model.

quency as the phase of microbridge 2. Thus the mean value of V_1 remains at zero as required by the Josephson equations. The slope of the I_2-$\bar{V}_2$ curve is changed during the interval when the potential of microbridge 1 is zero. This effect is displayed in Fig. 6 for $\alpha = 0.5$, $\delta = 0.667$, $I_{c1} = 0.2$, $I_{c_2} = 1.8$, and $I_1 = 2.2$. The two limiting values of I_2 that make $V_1 = 0$ are given by

$$I_2 = \left[I_{c2}^2 + \left(\frac{I_1 \pm I_{c_1}}{\alpha} \right)^2 \right]^{1/2}. \tag{5}$$

These values are indicated on Fig. 6 and they provide a method of obtaining values of α from experimental data when numerical values of I_{c1} and I_{c2} are known.

EXPERIMENTAL RESULTS

In this section we describe experiments performed on thin-film microbridges which were strongly coupled and so exhibited some of the phenomena mentioned above. In order to fabricate such strongly coupled microbridges it is necessary to make the separation of the microbridges less than the quasiparticle diffusion length (which is of the order of 6 μm for tin). A new technique for preparing closely coupled microbridges was developed and is described here. A Sn-SiO-Sn-SiO sandwich (Fig. 7) was evaporated onto a glass slide with the first Sn layer in contact with the glass. The slide was removed from the evaporator and mounted under an optical microscope in a helium atmosphere. A tungsten point that had been previously electroetched[21] so that its point had a diameter of less than 0.5 μm was mounted coaxially in a miniature free floating piston and this in turn was mounted in place of the objective lens. The microscope is used here only as a device for precisely lowering and raising the tip. The piston and tungsten point had a mass of 10 g and the point projected beyond the end of the piston toward the sandwich on the glass slide. The tungsten point was lowered onto the sandwich and the resistance between the tungsten

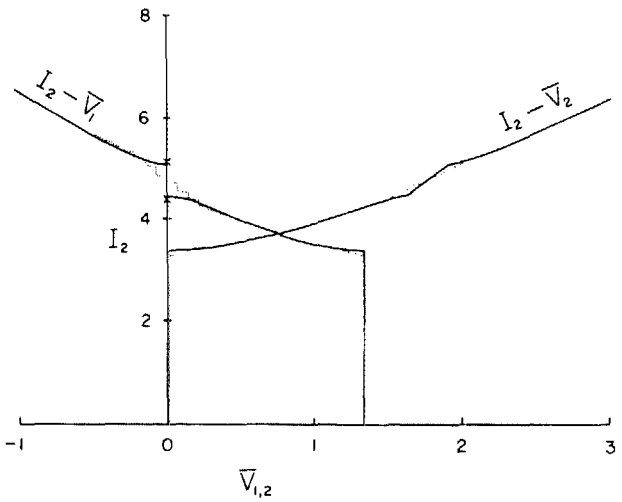

FIG. 6. Voltage characteristic from the analog simulator for $\alpha = 0.5$, $\delta = 0.667$, $I_1 = 2.2$, $I_{c1} = 0.2$, $I_{c2} = 1.8$, for the series aiding case at larger I_2 currents (continuous line). The dotted curve is the characteristic when an ac signal 100 Hz and peak curent in normalized units of value 1.0 is applied to each microbridge. The limits of the zero voltage current in the I_2-$\bar{V}_1$ curve that are predicted by Eq. (5) are indicated by ×'s.

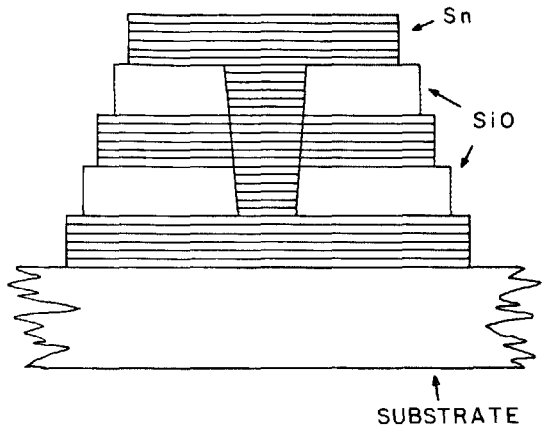

FIG. 7. A transverse schematic view of the coupled microbridges.

point and the lowest Sn layer was monitored with a circuit that had a maximum current of 60 μA. As soon as the resistance had dropped to less than 100 Ω the tungsten point was raised. The slide was returned to the evaporator and a final Sn layer was evaporated on top of the sandwich. The hole created by the tungsten point was filled by Sn during the evaporation of the final layer and where this hole passes through the two SiO layers the two microbridges are formed. Thus the separation of the two microbridges is equal to the thickness of the central Sn layer. The length of each microbridge is determined by the thickness of the SiO layers. The diameter of the microbridges is approximately equal to that of the tungsten point and should be less than the coherence length.

A coupled microbridge was fabricated by this method with the tin layers 1000 Å thick and the SiO layers 1000 Å thick. The resulting two microbridges had resistances of 0.09 and 0.18 Ω. The individual I-V characteristics are shown in Fig. 8. These curves were obtained by driving only one link at a time. Note, however, that these characteristics will not necessarily be identical to those of the isolated microbridge. The plots of I_2-$\bar{V}_2$ and I_2-$\bar{V}_1$ are shown in Fig. 9 for the series aiding case with $I_1 = 1.4$ mA at 3.62 K. The region where the potential of $\bar{V}_1$ goes to zero is clearly visible. The value of α calculated along the lines indicated by Jillie *et al.*[20] was found to be approximately 0.9.

At these large values of α it is possible for the beat frequency of the Josephson oscillators to have the same influence on each microbridge as that of external microwaves. In the series opposing mode and the series aiding mode the analog simulator revealed a step structure in the I-V characteristic as shown in Fig. 10. The step position changes as the bias current through microbridge 1 is varied. For the series opposing mode step positions are given by $\bar{V}_1/(\bar{V}_1 - \bar{V}_2) = n$ where n is an integer for the series opposing mode. For the series aiding mode, the step positions are given by $\bar{V}_1/(\bar{V}_2 - \bar{V}_1) = n$. The same type of structure was observed in the experimental I-V curves as shown in Fig. 9 but only for the series opposing case. That this step structure is caused by the beat frequency of the two Josephson oscillators can best be illustrated by observing, on the analog simulator, the time derivative of the phase. In Fig. 11 the time derivative of the

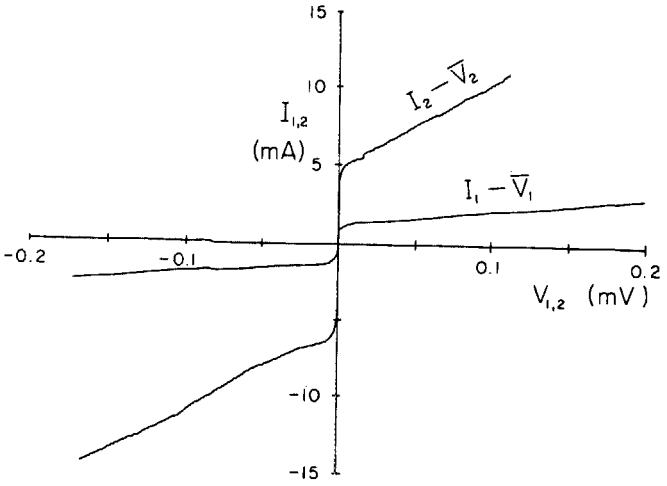

FIG. 8. Current-voltage characteristics for the individual microbridges of the coupled pair.

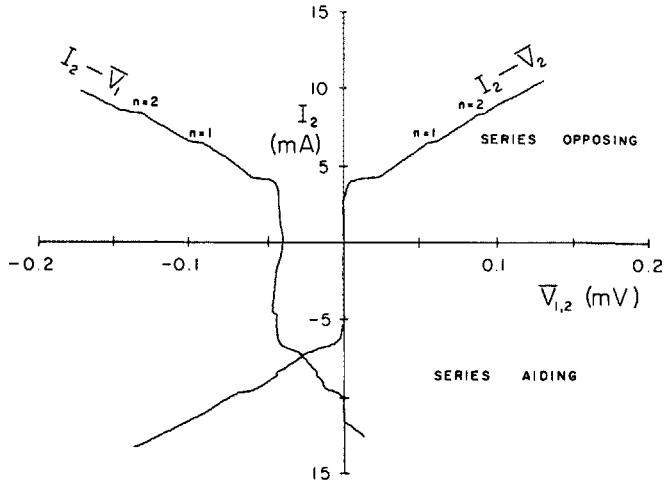

FIG. 9. I_2-$\bar{V}_2$ plot and the I_2-$\bar{V}_1$ plot for the coupled microbridges at 3.61 K and $I = 1.35$ mA.

phase of microbridge 1 is shown for various values of current I_2 and these values are indicated on the I_2-$\bar{V}_1$ characteristic of Fig. 10. The phase derivative shows a typical peaky appearance with the number of peaks increasing at each step of the I_2-$\bar{V}_1$ characteristic. When the current I_2 is sufficiently large that there are no steps, then the phase derivative takes on the appearance of a typical beat frequency [Fig. 11 (F)]. This beat frequency corresponds to the potential difference $\bar{V}_2$-$\bar{V}_1$ of the two microbridges. By way of comparison the I-V characteristic of a single isolated microbridge with microwaves, that was generated by the analog simulator, is given in Fig. 12 and the phase derivative of this microbridge for various currents are given in Fig. 13. There is much similarity between the phase derivatives of the single microbridge with microwaves and the phase derivative of the strongly coupled microbridge. The main difference occurs at large currents where the coupled microbridges yield a typical beat frequency appearance whereas the single microbridge with microwaves shows a phase derivative that is the addition of the Josephson frequency and the microwave frequency. It is possible to estimate a value of the beat frequency from the potential difference of the two microbridges, which was 0.23 in normalized units or 0.153 V. As the voltage to frequency conversion factor of the voltage controlled oscillator (VCO) is 13360 rad/sec V, the beat frequency is $13360 \times 0.153/2 = 325$ Hz. This is quite close to the observed value of the beat frequency, 333 Hz, estimated from Fig. 11 (F).

MICROWAVES

A study of the effect of microwaves on coupled microbridges can easily be carried out using the analog simulation. In a microbridge, microwaves manifest themselves as an ac current which can be simulated by adding an ac current to the summing point of the two op amps in Fig. 2. We have assumed that the same ac current is present at each microbridge. The voltage to frequency conversion factor of the analog simulator is 13360 rad/V sec so an input signal of 100

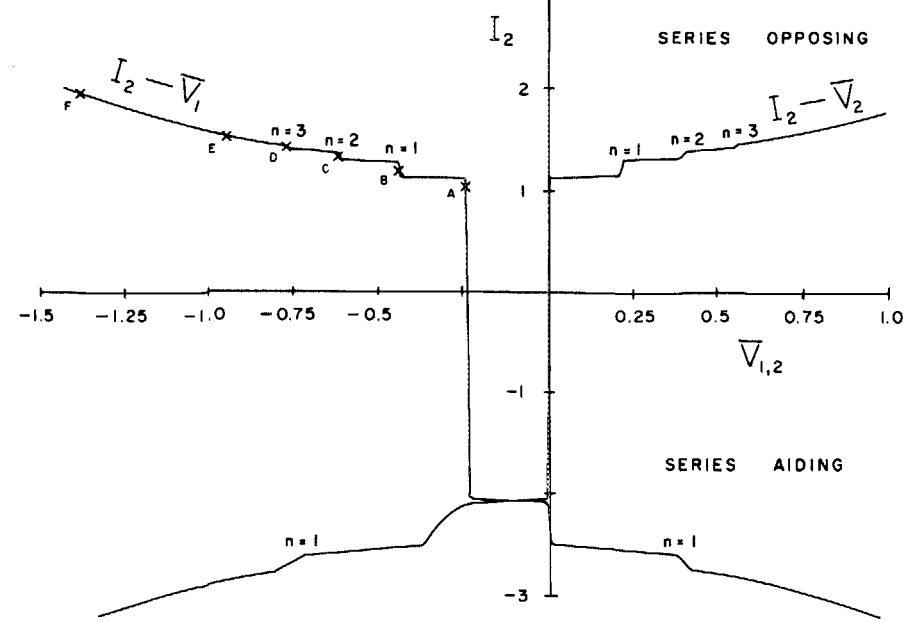

FIG. 10. Voltage characteristics from the simulator for $\alpha = 0.5$, $\delta = 0.667$, $I_{c_1} = 0.3$, $I_{c2} = 1.7$, $I_1 = 0.6$, $r_1 = 4.6k$, $r_2 = 3.06k$, $r_1' = r_2' = 5.11k$.

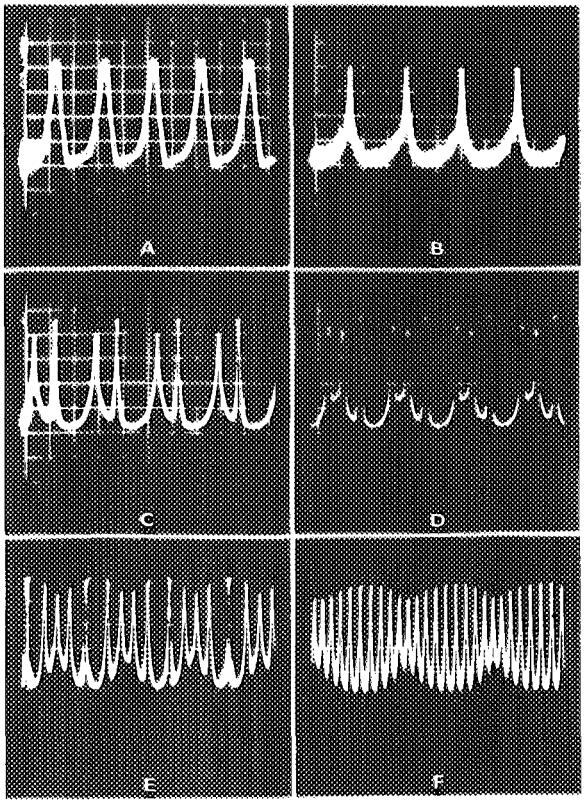

FIG. 11. V_1 vs time for various points on the I_2-$\bar{V}_1$ curve of Fig. 10.

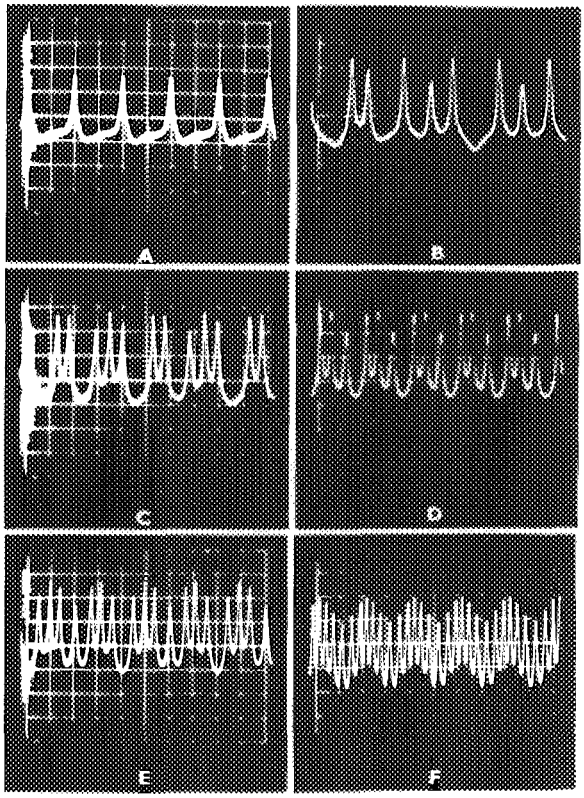

FIG. 13. V_1 vs time at various points of the I-$\bar{V}$ characteristic of Fig. 12.

Hz to the simulator is equivalent to a microwave frequency of $1.4695\times 10^{14}/V_0$ rad/sec. The results of the simulation for the series aiding case with $\alpha = 0.2$, $\delta = 0.667$, $I_{c1} = 1.2$, $I_{c2} = 0.8$, and $I_1 = 2$ are in Fig. 14. Typical steps appear at low voltages in the I_2-$\bar{V}_2$ curve which are equivalent to the steps that would be present in the I-V characteristic of a single microbridge. These steps are separated by a reduced voltage $2\pi f/k$ where f is the input frequency to the simulator. Similar steps occur in the I_2-$\bar{V}_1$ characteristic. These steps occur at the same currents as the steps in the I_2-$\bar{V}_2$ characteristic but they are not separated by constant voltage intervals. The center of each locking steps occurs when the difference of the frequencies of each microbridge is a multiple, nf, $(n = 0, -1, -2, \cdots)$ of the microwave frequency f. Following the work of Jain *et al.*[7] we have replotted this data in the form of I_2 vs $\bar{V}_2$-$\bar{V}_1$ in Fig. 5. The microwaves produce steps in this characteristic in an analagous way to the steps created in the I-V characteristic of a single microbridge when radiated by microwaves.

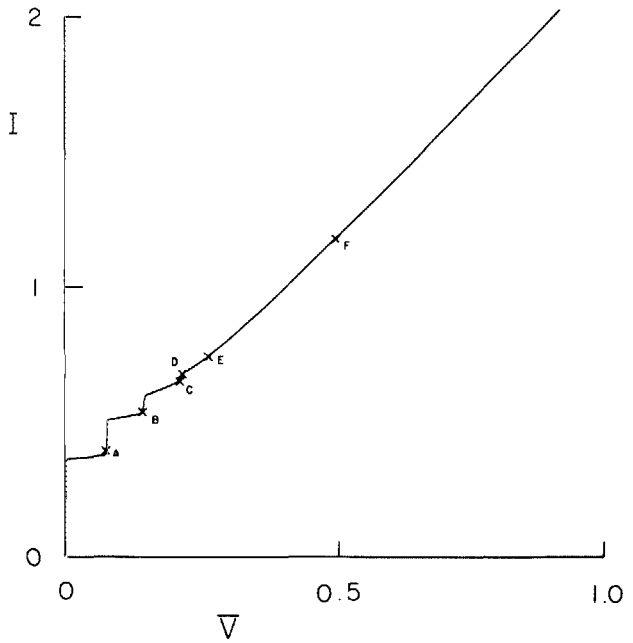

FIG. 12. I-$\bar{V}$ characteristic from the analog simulator for a single microbridge in the presence of a 100-Hz ac signal.

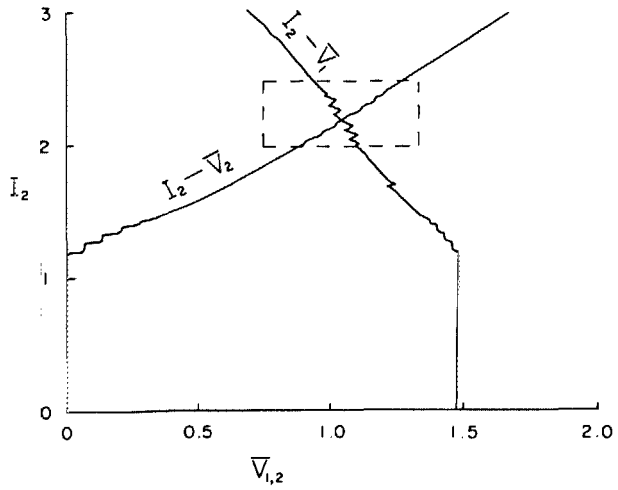

FIG. 14. I_2 vs $\bar{V}_2$ and $\bar{V}_1$ for the series aiding case and the same conditions as Fig. 3 but with an ac signal of 100-Hz input to each microbridge. The amplitude of the ac signal was 0.25 (normalized units).

The potential of microbridge 1 will reach zero for the current aiding case when I_2 is sufficiently large and this effect is shown in Fig. 6. The region around the zero voltage range of microbridge 1 is further modified when microwaves are present. Figure 6 shows the effect of a 100-Hz signal on the potential of microbridge 1. Steps are generated in the characteristic in a similar that steps are created in a single microbridge. The step separation is given by $2\pi f/k$ in reduced units.

SUMMARY

We have shown that an electronic analog simulator may be used to obtain solutions of the equations that represent superconducting microbridges coupled by quasiparticles. Our simulation solution and experimental data are in qualitative agreement. However, as the separation of the microbridges was less than the coherence length (about 0.23 μm in these microbridges) coupling due to order parameter modulation may be present. For very strong coupling several new phenomena are predicted. The beat frequency arising from the Josephson oscillations of the two individual microbridges will act in the same way as externally applied microwaves and cause steps to appear in the I-V characteristics. Strongly coupled superconducting microbridges were prepared by a new technique and the I-V characteristics of these confirm the step structure due to the Josephson oscillation beat frequency.

ACKNOWLEDGMENTS

The authors would like to acknowledge useful discussions with J. A. Blackburn and M. A. H. Nerenberg. This work was supported in part by a grant from the Natural Science and Engineering Research Council of Canada.

[1]D. E. McCumber, J. Appl. Phys. **39**, 3113 (1968).
[2]W. C. Stewart, Appl. Phys. Lett. **12**, 277 (1968).
[3]J. Matisoo, IBM J. Res. Develop. **24**, 113 (1980).
[4]T. D. Clark and P. E. Lindelof, Appl. Phys. Lett. **29**, 751 (1976).
[5]M. A. H. Nerenberg, J. A. Blackburn, and D. W. Jillie Phys. Rev. B **21**, 118 (1980).
[6]D. W. Jillie, M. A. H. Nerenberg, and J. A. Blackburn, Phys. Rev. B **21**, 125 (1980).
[7]A. K. Jain, K. K. Likarev, J. E. Lukens, and J. E. Sauvageau, Appl. Phys. Lett. **41**, 566 (1982).
[8]P. E. Lindelof and J. Bindslev Hansen, J. Low Temp. Phys. **29**, 369 (1977).
[9]W. Howard and Y. K. Kao, in *Proceedings of the Fourteenth International Conference on Low Temperature Physics, Otaniemi, Finland*, 1975, edited by M. Krusius and M. Vuorio (North-Hollywood, Amsterdam, 1975), Vol. 4, p. 144.
[10]Y. S. Way, K. S. Hsu, and Y. H. Kao, Phys. Rev. Lett. **39**, 1684 (1977).
[11]R. W. Henry, D. E. Prober, and A. Davidson Am. J. Phys. **49**, 1035 (1981).
[12]R. W. Henry, and D. E. Prober, Rev. Sci. Instrum. **52**, 902 (1981).
[13]C. K. Bak and N. F. Pedersen, Appl. Phys. Lett. **22**, 149 (1973).
[14]D. E. Prober, S. E. G. Slusky, R. W. Henry, and L. D. Jackel, J. Appl. Phys. **52**, 4145 (1981).
[15]Akiho Yagi and Itaru Kurosawa, Rev. Sci. Instrum. **51**, 14 (1981).
[16]K. H. Gundlach, J. Kadlec, and W. Heller, J. Appl. Phys. **48**, 1688 (1977).
[17]J. H. Magerlein, Rev. Sci. Instrum. **49**, 486 (1978).
[18]V. K. Kornev and V. K. Semenov, IEEE Trans. Magn. **MAG-19**, 633 (1983).
[19]A. K. Jain, K. K. Likarev, J. E. Lukens, and J. E. Sauvageau, Phys. Rept. (in press).
[20]D. W. Jillie, J. E. Lukens, and Y. H. Kao, Phys. Rev. Lett. **38**, 915 (1977).
[21]The tungsten points were prepared in the following way. A length of 36 AWG tungsten wire was electroetched in a 6N sodium hydroxide solution at room temperature and at 20-V dc potential. The tungsten was positive and the negative electrode was copper about 1 cm away. This procedure formed a coarse tip. The potential was changed to 14-V dc and then the tip was further electroeteched for 1 sec with only the tip in contact with the etching solution.